HHS Public Access

Author manuscript

Adv Healthc Mater. Author manuscript; available in PMC 2020 March 01.

Published in final edited form as:

Adv Healthc Mater. 2019 March ; 8(6): e1800854. doi:10.1002/adhm.201800854.

Gold Nanoparticles with Antibiotic-Metallopolymers toward Broad-Spectrum Antibacterial Effect

Peng Yang, **Parasmani Pageni**[†,¶], **Md Anisur Rahman**[†,¶], **Marpe Bam**[†], **Tianyu Zhu**[‡], **Yung Pin Chen**[†], **Mitzi Nagarkatti**[§], **Alan W. Decho**[‡,§], and **Chuanbing Tang**[*,†]

[†]Department of Chemistry and Biochemistry, University of South Carolina, Columbia, South Carolina 29208, United States

[‡]Department of Pathology, Microbiology and Immunology, University of South Carolina, School of Medicine, Columbia, South Carolina 29209, United States

[§]Department of Environmental Health Sciences, Arnold School of Public Health, University of South Carolina, Columbia, South Carolina 29208, United States

Abstract

Bacterial infection has evolved into one of most dangerous global health crises. Designing potent antimicrobial agents that can combat drug-resistant bacteria is essential for treating bacterial infections. In this report, we developed a strategy to graft metallopolymer-antibiotic bioconjugates on gold nanoparticles as an antibacterial agent to fight against different bacterial strains. Thus, these nanoparticle conjugates combined various components in one system to display enhanced bactericidal efficacy, in which small sized nanoparticles provide high surface area for bacteria to contact, cationic metallopolymers interact with the negatively-charged bacterial membranes, and β-lactam antibiotics are improved their sterilization capabilities via evading intracellular enzymolysis by β-lactamase. This nanoparticle-based antibiotic-metallopolymer system exhibited excellent broad-spectrum antibacterial effect, particularly for Gram-negative bacteria, due to the synergistic effect of multi-components on the interaction with bacteria.

TOC Graphic

[*]**Corresponding Author** tang4@mailbox.sc.edu.

[¶]Author Contributions

P. Yang, and P. Pageni equally contributed to this work.

Notes

The authors declare no competing financial interest.

Supporting Information

Details of the antimicrobial experimental procedures and other characterization data is available from the Wiley Online Library or from author.

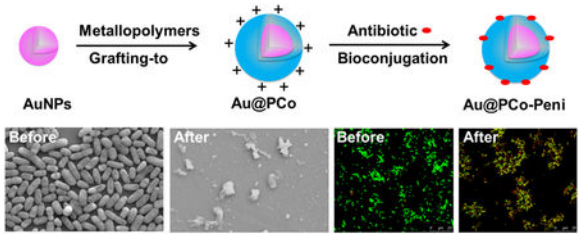

Metallopolymer-antibiotic bioconjugates on gold nanoparticles are synthesized by a "grafting-to" approach and a bioconjugation process. These nanoparticles can be used as antibacterial agents to enhance the activity of β-lactam antibiotics and fight against different strains of Gram-positive and Gram-negative bacteria.

1. Introduction

Bacterial infection is one of the most dangerous health crises the word is facing. The consequences includes increased healthcare cost, destruction of local tissues, patient disability, morbidity, and even death.[1-3] According to a study on antimicrobial resistance in 2014,[4] bacterial infections currently cause at least 50,000 deaths annually across the US and Europe, with significantly higher numbers in other areas. If more-effective strategies are not taken to prevent and treat bacterial infections, it has been predicted that by 2050 infections could claim 10 million lives with costs approaching $100 trillion (USD) dollars worldwide.[5] However, commonly-used antibiotics, such as penicillin and methicillin, have diminished antimicrobial efficacies and/or are ineffective against numerous multidrug-resistant (MDR) bacterial pathogens because of overuse of these drugs for so many years. [5, 6] Therefore, resurrecting the activity of conventional antibiotics or designing other potential antibacterial compounds that combat drug-resistant bacteria is essential for treating bacterial infections. [7, 8]

In recent years, cationic compounds and polymers,[9-11] such as quaternary ammonium,[12-14] phosphonium compounds,[15] and peptides,[16, 17] have garnered a great deal of attention as antimicrobial agents because of their ability to adsorb onto the negatively-charged bacterial cell surfaces and to insert their hydrophobic groups into membranes to combat bacteria. But many of these antibacterial compounds showed cytotoxicity on mammalian cells and could induce apoptosis via physical damage, thus limiting their clinic applications. [10] Recently, we reported a class of non-cytotoxic antimicrobial cationic metallopolymers,[18, 19] which could form bioconjugates with conventional β-lactam antibiotics, such as penicillin, amoxicillin and cefazolin, via unique ion-pairs between cationic metallocenium moieties and carboxylate anions. The bioconjugates efficiently protected β-lactam antibiotics from hydrolysis by a β-lactamase enzyme in bacteria and lysed different strains of methicillin-resistant *Staphylococcus aureus* (MRSA).

Compared with antibiotic molecules or polymers, nanoparticles (NPs) offer the possibility to attain better bactericidal and therapeutic effects because of their unique physical properties. [20-23] For instance, the size of NPs is very small (<100 nm), which can improve their ability to penetrate membranes of bacteria (>1μm) and penetrate bacteria easily.[24-27] The high

surface area of NPs favors high loading capacity of small molecular antibiotics, increasing the enrichment of antibiotics in the target bacteria.[28-31] The inherent features of gold nanoparticles (Au NPs) provide advantages of small size, large surface area, straightforward surface modification by thiols and amines, not being the substrate of bacterial efflux pumps, and the safety approval by U.S. FDA, which allow Au NPs to be useful as antibacterial agents.[32-39]

Herein, we developed a strategy to fight against different strains of Gram-positive and Gram-negative bacteria by presenting metallopolymer-antibiotic bioconjugates on gold nanoparticles as an antibacterial agent to further enhance the activity of conventional β-lactam antibiotics. A variety of characterization techniques, including transmission electron microscopy (TEM), dynamic light scattering (DLS), thermal gravimetric analysis (TGA), Zeta-potential analysis, UV-visible spectra, and ^{1}H NMR spectra, were performed systematically to determine the formation of Au@PCo NPs (cobaltocenium polymers coating on Au NPs). After bio-conjugating with β-lactam antibiotics penicillin-G, the Au@PCo-Peni NPs showed enhanced antibacterial efficacy on both Gram-positive and Gram-negative bacteria, compared with PCo-Penicillin conjugates and penicillin-G alone. Confocal laser scanning microscopy (CLSM), scanning electron microscopy (SEM) and TEM indicated that Au@PCo-Peni NPs can penetrate bacteria membranes and destroy their permeability, causing the bacterial death.

2. Results and discussion

The cationic cobaltocenium homopolymer (PCo) was first synthesized via reversible-addition fragmentation chain transfer (RAFT) polymerization[40, 41] using 2-cobaltocenium amidoethyl methacrylate hexafluorophosphate ($CoAEMAPF_6$) as a monomer and 2-Cyano-2-propyl benzodithioate (CPB) as a chain transfer agent (CTA) (Scheme 1a). The PCo homopolymer showed excellent water-solubility after its ligand exchanging from from PF_6^- to Cl^- using tetrabutylammonium chloride (TBACl) as a phase-transfer ion-exchange reagent.[42] Then, the dithioester end groups of RAFT agent in PCo polymer were reduced to thiol groups by $NaBH_4$ in aqueous media at ambient temperature. The thiol end-capped PCo could be coated on Au-NPs to form Au@PCo nanoparticles by a “grafting-to” approach.[43] Finally, a bioconjugate between cationic PCo and anionic β-lactam antibiotics such as penicillin-G could prevent the hydrolyzation of β-lactam by β-lactamase(s) and thus improve the sterilization capability of antibiotics.

Compared with ^{1}H NMR spectrum of $CoAEMAPF_6$ monomer (Figure S1a), the vinyl proton signals from methacrylate double bond at ~6.10 and ~5.70 ppm disappeared in PCo polymers (Figure S1b). Meanwhile, the three peaks at ~6.25 to ~5.80 ppm corresponding to the cyclopentadienyl (Cp) rings of the cobaltocenium unit remained, indicating the successful polymerization of cobaltocenium monomer. The NMR spectra were further used to track the conversation of $CoAEMAPF_6$ monomer during the polymerization process and determine the final molecular weight of PCo homopolymers. Three PCo homopolymers with different molecular weights, respectively, 6,000 g/mol (noted as PCo-6K), 15,000 g/mol (PCo-15K), 30,000 g/mol (PCo-30K), were finally synthesized.

Au NPs were prepared using chloroauric acid as the precursor, tetrakis(hydroxymethyl)phosphonium chloride (THPC) as the reducing agent which could produce ultrafine gold particles.[44] TEM and DLS showed the diameter of Au NPs was about 2-3 nm (Figure 1a and S2). After coating PCo polymers with different molecular weight, we obtained three sets of Au@PCo NPs (referred to as Au@PCo-6K, Au@PCo-15K and Au@PCo-30K). TEM images indicated all Au@PCo NPs had good dispersions (Figure 1b-d). As expected, the size of Au@PCo NPs increased to ~4 nm (Au@PCo-6K), 6 nm (Au@PCo-15K) and 9 nm (Au@PCo-30K), respectively, with the increase of molecular weight of PCo polymers. DLS analysis further confirmed the increased sizes of Au@PCo NPs under different polymer molecular weight as shown in Figure S2. The successful surface functionalization of gold nanoparticles with cationic cobaltocenium ligands was also analyzed by Zeta-potential analysis, UV-vis spectra and ^{1}H NMR spectra. Compared to the negative zeta potential of Au NPs at −26 eV, the potential of Au@PCo NPs increased to about +40 eV (Figure S3). The UV-visible absorption of Au NPs only had a broad shoulder under the ultraviolet region, while the spectrum of Au@PCo NPs showed an obvious absorption peak of cobaltocenium polymer at 280 nm (Figure S4). The three characteristic peaks from ~6.25 to ~5.80 ppm corresponding to the Cp rings of cobaltocenium were also found in the ^{1}H NMR spectrum of Au@PCo NPs (Figure S5), indicating the successful grafting of cobaltocenium polymers onto Au NPs. Thermal gravimetric analysis (TGA) data suggested that the weight percentage of cobaltocenium polymers in the Au@PCo NPs is about 43% (Au@PCo-6K), 38% (Au@PCo-15K), and 27% (Au@PCo-30K), respectively (Figure S6).

We first evaluated antimicrobial activities of Au NPs, PCo and Au@PCo NPs against Gram-positive bacteria *S. aureus* and Gram-negative bacteria *K. pneumonia* using disk-diffusion assays. The inhibition zone was examined to verify the bactericidal of these antimicrobial agents by measuring the diameter of the clear zone around the disk with a vernier caliper. As expected, Au NPs alone could not inhibit the proliferation of *S. aureus* and *K. pneumonia* even at high concentration (Figure S7). Compared with PCo-15K homopolymers, the Au@PCo-15K NPs showed significantly enhanced activities against both *S. aureus* (Figure S7a) and *K. pneumonia* at different concentrations (Figure S7b). However, there was more significant molecular weight-dependent response on bacterial proliferation for PCo homopolymers than that for the Au@PCo NPs. For example, the PCo-15K homopolymers displayed the biggest inhibition zone against both *S. aureus* (Figure S7c) and *K. pneumonia* (Figure S7d) compared with PCo-6K and PCo-30K homopolymers. While the Au@PCo-15K NPs also exhibited the highest antimicrobial activity, the difference of activities among these three Au@PCo NPs was very small, especially for Gram-negative bacteria *K. pneumonia.* The minimum inhibitory concentration (MIC) values of cationic cobaltocenium polymers (PCo) and Au@PCo NPs with different molecule weight of cobaltocenium polymers against Gram-positive *S. aureus* and Gram-negative *K. pneumonia* are summarized in Table S1 in supporting information. As for *S. aureus*, the MIC value of PCo-15K was about 100 μg/mL, which is much lower than the values of PCo-6K (136 μg/mL) and PCo-30K (121 μg/mL). Furthermore, the MICs of Au@PCo-15K NPs against *S. aureus* decreased to 58 μg/mL, in comparison to 95 μg/mL for Au@PCo-6K NPs and 76 μg/mL for Au@PCo-30K NPs. For *K. pneu*monia, the Au@PCo-15K NPs has the lowest

MIC value of 49 μg/mL, which was a little lower than that of Au@PCo-6K NPs (53 μg/mL) and Au@PCo-30K NPs (61 μg/mL).

In order to further enhance the antimicrobial activity of Au@PCo NPs, we then chose penicillin-G as a model β-lactam antibiotic to study its bioconjugate with Au@PCo-15K NPs (labeled as Au@PCo-Peni), which was easily formed via ionic complexation between anionic carboxylate ions of penicillin-G and cationic cobaltocenium moiety of PCo in Au@PCo NPs. TGA data (Figure S8) suggested that the weight percentage of penicillin-G in the Au@PCo-Peni NPs was about 27%, with a molar ratio of penicillin-G to cobaltocenium at ~ 0.8:1. The sterilization capability of Au@PCo-Peni bioconjugates were evaluated against different strains of bacteria including one Gram-positive bacterium (*S. aureus*) and three Gram-negative bacteria (*E. coli*, *K. pneumoniae* and *P. aeruginosa*) by disk-diffusion assays. A bioconjugate containing polycobaltocenium homopolymer (15,000 g/mol) and penicillin-G (i.e. PCo-Peni, with 30wt% penicillin-G) was used as a control group. Initially, various amount of penicillin-G ranging from 5 μg to 15 μg was tested. As shown in Figure 2a, penicillin-G at the amount of 5 μg displayed minimal efficacy in killing Gram-negative bacterium *S. aureus*. By contrast, PCo-Peni and Au@PCo-Peni bioconjugates exhibited higher antibacterial efficacy at the same amount of penicillin-G, with the inhibition zone increasing to 11 mm and 14.5 mm, respectively. As expected, the antibacterial efficacy of penicillin-G, PCo-Peni, and Au@PCo-Peni significantly increased with the adding amount of penicillin-G. When the amount of penicillin-G increased to 10 and 15 μg, the inhibition zone of Au@PCo-Peni increased to 19 and 21 mm, respectively, which were both bigger than penicillin-G (9.5 and 15 mm) and PCo-Peni (15 and 20 mm). For Gram-negative bacteria, penicillin-G showed much lower antimicrobial activity as compared to Gram-positive bacteria. As shown in Figure 2a ii-iv, it is hardly to see clear inhibition zone for 10 μg penicillin-G against all three Gram-negative bacteria. This is because Gram-negative bacteria possessed two different cell membranes, which would block the entry of antibiotics into bacteria via a series of protection mechanisms. Using nanoparticles as antimicrobial agents could increase the permeability of bacterial membranes and enhance antimicrobial activity against Gram-negative bacteria. As shown in Figure 2a, Au@PCo-Peni NPs exhibited the strongest antimicrobial activities against all three Gram-negative at different amount of penicillin-G.

To better quantify the inhibition efficacy of Au@PCo-Peni NPs, bacteria were incubated with different antimicrobial agents in tryptic soy broth (TBS) solution for 8 h. Then, bacterial growth was detected with OD_{600} (Figure 2b) and inhibitory percentages (Figure 2c) were calculated, compared to the control groups, which were TSB solutions of four different bacteria without any antimicrobial agents. As for *S. aureus*, the OD_{600} value of Au@PCo-Peni NPs was only 0.03, which was approximately 55 times lower than that of the control (1.65), 13 times lower than penicillin-G (0.39), and 8 times lower than PCo-Peni (0.25), respectively (Figure 2b). The inhibitory efficiency of Au@PCo-Peni against *S. aureus* increased to 98.5% from 84.5% (PCo-Peni) and 76.8% (the control) (Figure 2c). The similar antibacterial trends and inhibitory efficiency were also found for other Gram-negative bacteria, which was consistent with the results from the disk-diffusion assays. Table 1 showed the MIC values of Au@PCo-Peni NPs, PCo-Peni conjugates and penicillin-G against these four different bacteria. All MIC values of Au@PCo-Peni NPs and PCo-Peni

conjugates were calculated based on the effective penicillin concentration in their conjugates. The MIC value of Au@PCo-Peni NPs was about 2.6 μg/mL against gram-positive *S.aureus*, which was much lower than the values of penicillin-G (15.8 μg/mL) and PCo-Peni conjugates (6.4 μg/mL). Furthermore, MIC values of Au@PCo-Peni NPs against Gram-negative bacteria were almost 4~5 times and 2~3 times less than that of penicillin-G and PCo-Peni conjugates, respectively.

The kinetics of antibacterial activity of Au@ PCo-Peni NPs was investigated. The aqueous Au@ PCo-Peni NPs solution (30 μL) with the concentration of MIC was added to 96-well plates. All assays were carried out in duplicate from the same assay plate. Then, 170 μL bacterial TSB solution ($OD6_{00}$=1.00) was added to the wells. The bacterial TSB solution without conjugates was used as the control. The OD_{600} values of bacterial solution were checked at a time interval of 0 h, 1 h, 2 h, 4 h, 6 h, 8 h, 12h, and 24 h. As shown in Figure S9 in supporting information, Au@ PCo-Peni NPs killed bacteria almost instantaneously, which can be seen by the reduction of OD_{600} values from 1.0 to 0.88 after 1 h, while OD_{600} values of bacteria in the control group increased to 1.1. The remarkable antimicrobial efficiency happened between 4 h and 12h, with OD_{600} values significantly decreasing to 0.2 for both *S. aureus* and *E. coli.* The bacteria could be completely killed in 24 h.

The inhibition effects of Au@PCo-Peni NPs against the four strains of bacteria were further visualized by confocal laser scanning microscopy (CLSM), scanning electron microscopy (SEM) and transmission electron microscopy (TEM). The bacteria were firstly stained by LIVE/DEAD BacLight dye (Bacterial Viability Kit; Invitrogen Inc.) and then checked their viability via CLSM (Figure 3a). The results of CLSM indicated the Au@PCo-Peni NPs almost killed all bacteria, with CLSM micrographs exhibiting strong yellow or red fluorescence from dead bacteria, however, the strong green fluorescence standing for live bacteria was observed in control groups. From FESEM images (Figure 3b), we found the bacterial membranes were disrupted totally by Au@PCo-Peni NPs, producing lots of cell fragments and shrunken dead cells, while the bacteria in control groups displayed an integrated rod or spherical morphology with a smooth surface. TEM further showed Au@PCo-Peni NPs aggregated around bacterial membranes and could penetrat bacteria, making the outer bacterial membranes destroyed, while the control bacterial cells kept intact and smooth surfaces. **(Figure 5)**. All these studies suggested the Au@PCo-Peni NPs have excellent antimicrobial efficiency against broad-spectrum bacteria.

The high bactericidal ability of Au@PCo-Peni NPs was mainly due to the synergistic effect of three aspects: i) the cationic cobaltocenium motif can interact with the negatively-charged bacterial membrane, making Au@PCo-Peni NPs attach to the surface of bacteria more closely; ii) the small sizes of Au@PCo-Peni NPs provided larger bacterial contact area to enhance their permeability into membranes and penetrate bacteria more easily; iii) once NPs enter bacterial cells, the cobaltocenium motif would release penicilin-G and bind β-lactamase, which can block the electrostatic chelation between penicillin-G and amino acid residue of β-lactamase, preventing the hydrolyzation of β-lactam in penicilin-G by β-lactamase(s) in bacteria and thus improving the sterilization capability of penicilin-G. Finally, the toxicity of Au@PCo NPs was analyzed on red blood cells (RBCs) by evaluating their capability to cause hemolysis of RBCs. Compared with the negative control group

(Triton 10X), the Au@PCo NPs rarely led to the lysis of RBCs (< 10%), even at a high concentration of 500 μg/mL (Figure S10), suggesting low cytotoxicity to mammalian cells.

3. Conclusions

We have developed a strategy to attach metallopolymer-antibiotic bioconjugates on gold nanoparticles as an antibacterial agent to fight against different strains of Gram-positive and Gram-negative bacteria. The thiol end-capped cobaltocenium polymers could be easily coated on Au nanoparticles to form Au@PCo NPs by a "grafting-to" approach. After bio-conjugating with an anionic β-lactam antibiotic penicillin-G, the formed cationic Au@PCo-Peni NPs with a small size and a large contact area can attach to the membranes of bacteria more closely, improve the vitality of penicillin-G and kill bacteria more effectively. We hope these multifunctional metallopolymer-based nanoparticles could be further explored in combating clinic infections by the pathogens resistant to conventional antibiotics.

4. Experimental section

Characterization:

^{1}H NMR spectra were carried out on a 400 MHz NMR spectrometer (Varian Mercury) using tetramethylsilane (TMS) as an internal reference. Dynamic light scattering (DLS) and Zeta-potential were recorded on a Nano-ZS instrument, model ZEN 3600 (Malvern Instruments). UV–vis spectra were operated on a UV-2450 spectrophotometer (Shimadzu) using a monochromatic light of various wavelengths over a range of 190–900 nm as light source and a 10.00 mm quartz cuvette as test vessel. Field-Emission Scanning Electron Microscopy (FE-SEM, Zeiss UltraPlus) was used to take images of bacterial cells after incubating overnight with test drugs. The samples were firstly coated with gold using Denton Dest II Sputter Coater for 45 s and then observed by SEM. A Hitachi 8000 transmission electron microscope (TEM) was applied to take images at an operating voltage of 150 kV. TEM samples were prepared by dropping solution on carbon-supported copper grids and then dried before observation.

Materials and Methods:

The monomer 2-Cobaltoceniumamidoethyl methacrylate hexafluorophosphate ($CoAEMAPF_6$) was prepared according to our earlier report.[40] 2-Aminoethyl methacrylate hydrochloride (90%), 4-(dimethylamino) pyridine tetrabutylammonium chloride (TBACl), and *N*-(3-dimethylaminopropyl)-*N*′-ethylcarbodiimide hydrochloride (EDC-HCl, 98%) were purchased from Sigma Aldrich and used as received. Tetrakis(hydroxymethyl)phosphonim chloride (referred to hereafter as THPC) was an 80% aqueous solution (practical grade) from Fluka, chloroauric acid (hydrogen tetrachloroaurate(III)) was from Johnson Matthey, assayed at 49.42 %. All the bacteria were obtained from ATCC company: *Staphylococcus aureus* (*S. aureus*, ATCC-33591), *Escherichia coli* (*E. coli*, ATCC-11775), *Klebsiella pneumoniae* (*K. pneumoniae*, ATCC-35596), and *Pseudomonas aeruginosa* (*P. aeruginosa*, ATCC-10145). Nitrocefin was purchased from TOKU-E and used as received. Azobisisobutyronitrile (AIBN) was was purchased from VWR and recrystallized from methanol. Sodium salt of penicillin-G was

purchased from VWR and 2-Cyano-2-propyl benzodithioate (CPB) was purchased from Strem Chemical Inc. Water was purified using Thermo Scientific Nanopure with ion conductivity at 18.2 MΩ. All other chemicals were from commercial sources and used as received.

Synthesis of poly(cobaltocenium (PCo) homopolymers:

Poly(cobaltocenium (PCo) homopolymers were prepared via reversible addition-fragmentation chain transfer (RAFT) polymerization:[40] Monomer CoAEMAPF_6 (490 mg, 1.0 mmol), initiator AIBN (0.5mg, 0.003mmol) and CTA agent CPB (3.5 mg, 0.01 mmol) were dissolved in DMF solution (1.0 mL) in a 10 mL Schlenk flask.. The mixture was degassed by purging N_2 for 30 min and then initiated at 90 °C for 1-2 h. After reaction, the PCo homopolymers with PF_6^- ligand were obtained by precipitation in cold dichloromethane. Finally, The PCo homopolymer showed excellent water-solubility after its ligand exchanging from from PF_6^- to Cl^- using tetrabutylammonium chloride (TBACl) as a phase-transfer ion-exchange reagent.[42] 1 mL acetonitrile solution of PCo homopolymers with PF_6^- ligand (30 mg/mL) was slowly dropped into 5 mL TBACl acetonitrile solution under vigorous stirring. After five minutes, the Cl^- paired PCo homopolymers with Cl^- ligand was precipitated and washed three times using acetonitrile to remove excess TBACl and remaining PF_6^- ions.

Synthesis of Au@PCo Nanoparticles:

Gold nanoparticles were synthesized according to a reported method.[44] In a 100-mL round-bottomed flask , while stirring, with 45.5 mL of water and then, in order, portions of aqueous solutions of sodium hydroxide (0.2 M, 1.5 mL), the reducing agent THPC (1 mL of a solution of 1.2 mL of 80% aqueous solution diluted to 100 mL with water), and the metal salt chloroauric acid (2 mL of dark-aged stock solution, 25 mM) results in the formation of orange-brown hydrosols of gold nanoparticles. The Au@PCo nanoparticles were prepared as following[43]: the PCo polymer (50 mg) was added to above gold NPs solution. Then, 1M $NaBH_4$ (2 mL) was added dropwise and the mixture was allowed to continue stirirng at room temperature for 48h. The mixture was centrifuged for 1h at 13000 rpm. the Au@PCo nanoparticles were got after centrifuge and rinsing with water for 3 times.

Synthesis of Au@PCo-Peni Nanoparticles:

Au@PCo NPs (15 mg) and penicillin-G sodium salt (10 mg) were first dissolved in 1 mL deionized water and stirred for 12 h. Then, the mixture was transferred into a dialysis bag (molecular weight cut off 3,000) and dialyzed against 3 L deionized water for 12 h.. The Au@PCo-Peni nanoparticles were collected via freeze-dry of above mixture.

Evaluation of antibacterial effects:

All bacteria were obtained from ATCC company: *Staphylococcus aureus* (*S. aureus*, ATCC-33591), *Klebsiella pneumoniae* (*K. pneumoniae*, ATCC-35596), *Escherichia coli* (*E. coli*, ATCC-11775), and *Proteus vulgaris* (*P. vulgaris*, ATCC-33420). A single colony of each bacterium was inoculated in 30 mL Tryptic Soy broth (TSB) solution at 37 °C and

shake at 190 rpm/min for 24 h. When the OD_{600} value of bacteria was about 1.00, suggesting bacteria with an optical density for further use.

For the agar disk-diffusion assays, each strain of bacteria was actively cultured on a mannitol salt agar (MSA), which was placed on a TSB agar plate. 10 μL 1.0×10^6 CFU/mL bacteria TBS solution was diluted to 1 mL, and then 100 μL diluted bacteria solution was spread on the surface of TSB agar plate to form a bacterial lawn. Then, the filter discs with 6 mm diameter were placed on the surface of TSB agar plate. Different amounts of Au@PCo-Peni NPs, PCo-Peni bioconjugates, Au@PCo NPs and Penicillin-G were dissolved in 30 μL water and then dropped to the filter discs. The plates were incubated in the oven for 18 h at 28 °C. A clear inhibition zone around the disk was developed, suggesting the antibacterial ability of these compounds.

Minimum inhibitory concentrations (MIC):

MIC values of antimicrobial agents against different bacteria were tested as follow method. The antimicrobial agents with different amounts was dissolved in water and added to 96-well plates (50 μL per well). Then, 150 μL TSB solution of bacteria was added to each well in above 96-well plates. The TSB solution of bacteria without antimicrobial agents was selected as the control group. These plates were shakily incubated for 12 hours at 37 °C. was detected at OD_{600} values were measured to detect the bacterial growth. All assays were measured twice in the same 96-well plate. Percentage inhibition were calculated by following equation:

$$\text{Inhibition } \% = \frac{OD_{600}{}^{(t)} - OD_{600}{}^{(0)}}{OD_{600}{}^{(t)}{}_c - OD_{600}{}^{(0)}{}_c}$$

Here, OD_{600} (t) indicates the OD_{600} value of bacteria after incubation with antimicrobial agents for t hours, OD_{600} (0) is the initial OD_{600} value of bacteria. OD_{600} $(t)_c$ indicates the OD_{600} value of control groups after incubation for t hours and OD_{600} $(0)_c$ is the initial OD_{600} value of control group.

LIVE/DEAD bacterial viability assays:

The four strains of bacteria were inoculated via a similar procedure used for MIC studies. 18.5 μg Au@PCo-Peni NPs (penicillin-G weight: 5μg) was added to 1 mL bacteria TBS solution with OD_{600} of 1.00. The bacteria TSB solution without antimicrobial agents was selected as the control group. After incubation for 18 h at 37 °C, the bacteria were stained by 1 μL LIVE/DEAD BacLight dye. The bacteria were fluorescence imaged using a confocal laser scanning microscopy (Leica TCS SP5) with a 63X oil immersion lens. Excited at 488 nm using Helium/Neon and Argon laser, the live bacteria showed green fluorescence with emission at 500 nm, while the dead bacteria displayed red fluorescence with emission at 635 nm because of the disrupted cell membranes.

Bacterial morphology assays:

The morphologies of bacterial strains treated by Au@PCo-Peni NPs were further visualized by scanning electron microscopy (SEM) and transmission electron microscopy (TEM). 18.5

μg Au@PCo-Peni NPs (penicillin-G weight: 5μg) was added to 1 mL bacteria TBS solution with OD_{600} of 1.00. The solution was added to a 12-well plate containing on one glass slide in each well and cultured overnight at 37 °C. The bacteria TSB solution without antimicrobial agents was selected as the control group. The glass slides covered by bacteria were first-fixed with 2.5% glutaraldehyde cacodylate buffer solution (pH = 7.2) for 3 h at 4 °C and post-fixed with 1% osmium tetraoxide buffer solution (pH = 7.2) for 1 h at 4 °C. After samples dry, they were sprayed with gold for 2 min using a sputter coater (Denton Dest II) and observed by FE-SEM (Zeiss UltraPlus). For TEM test, the bacteria TBS solution was dropwise added onto carbon-supported copper grids and then fixed by 2.5% glutaraldehyde cacodylate buffer solution and 1% osmium tetraoxide buffer solution before observation.

Supplementary Material

Refer to Web version on PubMed Central for supplementary material.

ACKNOWLEDGMENTS

The support from National Institutes of Health (R01AI120987) is acknowledged.

References

1. Hancock RE; Nijnik A; Philpott DJ, Modulating immunity as a therapy for bacterial infections. Nat. Rev. Microbiol. 2012, 10, (4), 243. [PubMed: 22421877]
2. Bierne H; Hamon M; Cossart P, Epigenetics and bacterial infections. Cold Spring Harb. Perspect. Med. 2012, 2, (12), a010272. [PubMed: 23209181]
3. Fernebro J, Fighting bacterial infections—future treatment options. Drug Resistance Updates 2011, 14, (2), 125–139. [PubMed: 21367651]
4. Curtis J; Yang S; Patkar N; Chen L; Singh J; Cannon G; Mikuls T; Delzell E; Saag K; Safford M, Risk of hospitalized bacterial infections associated with biologic treatment among US veterans with rheumatoid arthritis. Arthritis Care Res. 2014, 66, (7), 990–997.
5. Alanis AJ, Resistance to Antibiotics: Are We in the Post-Antibiotic Era? Arch. Med. Res. 2005, 36, (6), 697–705. [PubMed: 16216651]
6. Zhang Q-Q; Ying G-G; Pan C-G; Liu Y-S; Zhao J-L, Comprehensive evaluation of antibiotics emission and fate in the river basins of China: source analysis, multimedia modeling, and linkage to bacterial resistance. Environ. Sci. Technol. 2015, 49, (11), 6772–6782. [PubMed: 25961663]
7. Sterling SA; Miller WR; Pryor J; Puskarich MA; Jones AE, The impact of timing of antibiotics on outcomes in severe sepsis and septic shock: a systematic review and meta-analysis. Crit. Care Med. 2015, 43, (9), 1907. [PubMed: 26121073]
8. Cox LM; Blaser MJ, Antibiotics in early life and obesity. Nat. Rev. Endocrinol. 2015, 11, (3), 182. [PubMed: 25488483]
9. Yang Y; Cai Z; Huang Z; Tang X; Zhang X, Antimicrobial cationic polymers: From structural design to functional control. Polym. J. 2018, 50, (1), 33.
10. Engler AC; Wiradharma N; Ong ZY; Coady DJ; Hedrick JL; Yang Y-Y, Emerging trends in macromolecular antimicrobials to fight multi-drug-resistant infections. Nano Today 2012, 7, (3), 201–222.
11. Ganewatta MS; Tang C, Controlling macromolecular structures towards effective antimicrobial polymers. Polymer 2015, 63, A1–A29.
12. Jiao Y; Niu L.-n.; Ma S; Li J; Tay FR; Chen J.-h., Quaternary ammonium-based biomedical materials: State-of-the-art, toxicological aspects and antimicrobial resistance. Prog. Polym. Sci. 2017, 71, 53–90.

13. Asri LA; Crismaru M; Roest S; Chen Y; Ivashenko O; Rudolf P; Tiller JC; van der Mei HC; Loontjens TJ; Busscher HJ, A Shape-Adaptive, Antibacterial-Coating of Immobilized Quaternary-Ammonium Compounds Tethered on Hyperbranched Polyurea and its Mechanism of Action. Adv. Funct. Mater. 2014, 24, (3), 346–355.
14. Geng Z; Finn M, Thiabicyclononane-Based Antimicrobial Polycations. J. Am. Chem. Soc. 2017, 139, (43), 15401–15406. [PubMed: 29052422]
15. Hisey B; Ragogna PJ; Gillies ER, Phosphonium-functionalized polymer micelles with intrinsic antibacterial activity. Biomacromolecules 2017, 18, (3), 914–923. [PubMed: 28165737]
16. Fjell CD; Hiss JA; Hancock RE; Schneider G, Designing antimicrobial peptides: form follows function. Nat. Rev. Drug Discov. 2012, 11, (1), 37.
17. Narayana JL; Chen J-Y, Antimicrobial peptides: possible anti-infective agents. Peptides 2015, 72, 88–94. [PubMed: 26048089]
18. Zhang J; Chen YP; Miller KP; Ganewatta MS; Bam M; Yan Y; Nagarkatti M; Decho AW; Tang C, Antimicrobial metallopolymers and their bioconjugates with conventional antibiotics against multidrug-resistant bacteria. J. Am. Chem. Soc. 2014, 136, (13), 4873–4876. [PubMed: 24628053]
19. Yang P; Bam M; Pageni P; Zhu T; Chen YP; Nagarkatti M; Decho AW; Tang C, Trio Act of Boronolectin with Antibiotic-Metal Complexed Macromolecules toward Broad-Spectrum Antimicrobial Efficacy. ACS Infect. Dis. 2017, 3, (11), 845–853. [PubMed: 28976179]
20. Peng B; Zhang X; Aarts DG; Dullens RP, Superparamagnetic nickel colloidal nanocrystal clusters with antibacterial activity and bacteria binding ability. Nat. Nanotech. 2018, 1.
21. Li F; Lu J; Kong X; Hyeon T; Ling D, Dynamic nanoparticle assemblies for biomedical applications. Adv. Mater. 2017.
22. Lucky SS; Soo KC; Zhang Y, Nanoparticles in photodynamic therapy. Chem. Rev. 2015, 115, (4), 1990–2042. [PubMed: 25602130]
23. Zhang L; Pornpattananangkul D; Hu C-M; Huang C-M, Development of nanoparticles for antimicrobial drug delivery. Curr. Med. Chem. 2010, 17, (6), 585–594. [PubMed: 20015030]
24. Hajipour MJ; Fromm KM; Ashkarran AA; de Aberasturi DJ; de Larramendi IR; Rojo T; Serpooshan V; Parak WJ; Mahmoudi M, Antibacterial properties of nanoparticles. Trends Biotechnol. 2012, 30, (10), 499–511. [PubMed: 22884769]
25. Qi GB; Zhang D; Liu FH; Qiao ZY; Wang H, An “On-Site Transformation” Strategy for Treatment of Bacterial Infection. Adv. Mater. 2017, 29, (36).
26. Radovic-Moreno AF; Lu TK; Puscasu VA; Yoon CJ; Langer R; Farokhzad OC, Surface charge-switching polymeric nanoparticles for bacterial cell wall-targeted delivery of antibiotics. ACS Nano 2012, 6, (5), 4279–4287. [PubMed: 22471841]
27. Lam SJ; O’Brien-Simpson NM; Pantarat N; Sulistio A; Wong EH; Chen Y-Y; Lenzo JC; Holden JA; Blencowe A; Reynolds EC, Combating multidrug-resistant Gram-negative bacteria with structurally nanoengineered antimicrobial peptide polymers. Nat. Microbiol. 2016, 1, (11), 16162. [PubMed: 27617798]
28. Roy I; Shetty D; Hota R; Baek K; Kim J; Kim C; Kappert S; Kim K, A Multifunctional Subphthalocyanine Nanosphere for Targeting, Labeling, and Killing of Antibiotic-Resistant Bacteria. Angew. Chem. 2015, 127, (50), 15367–15370.
29. Song H; Ahmad Nor Y; Yu M; Yang Y; Zhang J; Zhang H; Xu C; Mitter N; Yu C, Silica nanopollens enhance adhesion for long-term bacterial inhibition. J. Am. Chem. Soc. 2016, 138, (20), 6455–6462. [PubMed: 27139159]
30. Chen J; Andler SM; Goddard JM; Nugen SR; Rotello VM, Integrating recognition elements with nanomaterials for bacteria sensing. Chem. Soc. Rev. 2017, 46, (5), 1272–1283. [PubMed: 27942636]
31. Nguyen T-K; Selvanayagam R; Ho KK; Chen R; Kutty SK; Rice SA; Kumar N; Barraud N; Duong HT; Boyer C, Co-delivery of nitric oxide and antibiotic using polymeric nanoparticles. Chem. Sci. 2016, 7, (2), 1016–1027. [PubMed: 28808526]
32. Pissuwan D; Niidome T; Cortie MB, The forthcoming applications of gold nanoparticles in drug and gene delivery systems. J. Control. Release 2011, 149, (1), 65–71. [PubMed: 20004222]

33. Chen WY; Chang HY; Lu JK; Huang YC; Harroun SG; Tseng YT; Li YJ; Huang CC; Chang HT, Self-Assembly of Antimicrobial Peptides on Gold Nanodots: Against Multidrug-Resistant Bacteria and Wound-Healing Application. Adv. Funct. Mater. 2015, 25, (46), 7189–7199.
34. Zhou Y; Kong Y; Kundu S; Cirillo JD; Liang H, Antibacterial activities of gold and silver nanoparticles against Escherichia coli and bacillus Calmette-Guérin. J. Nanobiotechnology 2012, 10, (1), 19. [PubMed: 22559747]
35. Abadeer NS; Murphy CJ, Recent progress in cancer thermal therapy using gold nanoparticles. J. Phys. Chem. C 2016, 120, (9), 4691–4716.
36. Feng ZV; Gunsolus IL; Qiu TA; Hurley KR; Nyberg LH; Frew H; Johnson KP; Vartanian AM; Jacob LM; Lohse SE, Impacts of gold nanoparticle charge and ligand type on surface binding and toxicity to Gram-negative and Gram-positive bacteria. Chem. Sci. 2015, 6, (9), 5186–5196. [PubMed: 29449924]
37. Tao Y; Ju E; Ren J; Qu X, Bifunctionalized mesoporous silica-supported gold nanoparticles: intrinsic oxidase and peroxidase catalytic activities for antibacterial applications. Adv. Mater. 2015, 27, (6), 1097–1104. [PubMed: 25655182]
38. Zhao Y; Tian Y; Cui Y; Liu W; Ma W; Jiang X, Small molecule-capped gold nanoparticles as potent antibacterial agents that target gram-negative bacteria. J. Am. Chem. Soc. 2010, 132, (35), 12349–12356. [PubMed: 20707350]
39. Bindhu M; Umadevi M, Antibacterial activities of green synthesized gold nanoparticles. Mater. Lett. 2014, 120, 122–125.
40. Zhang J; Ren L; Hardy CG; Tang C, Cobaltocenium-containing methacrylate homopolymers, block copolymers, and heterobimetallic polymers via RAFT polymerization. Macromolecules 2012, 45, (17), 6857–6863.
41. Yang P; Pageni P; Kabir MP; Zhu T; Tang C, Metallocene-Containing Homopolymers and Heterobimetallic Block Copolymers via Photoinduced RAFT Polymerization. ACS Macro Lett. 2016, 5, (11), 1293–1300. [PubMed: 29276651]
42. Zhang J; Yan Y; Chance MW; Chen J; Hayat J; Ma S; Tang C, Charged Metallopolymers as Universal Precursors for Versatile Cobalt Materials. Angew. Chem. Int. Ed. 2013, 52, (50), 13387–13391.
43. Lowe AB; Sumerlin BS; Donovan MS; McCormick CL, Facile preparation of transition metal nanoparticles stabilized by well-defined (co) polymers synthesized via aqueous reversible addition-fragmentation chain transfer polymerization. J. Am. Chem. Soc. 2002, 124, (39), 11562–11563. [PubMed: 12296698]
44. Duff DG; Baiker A; Edwards PP, A new hydrosol of gold clusters. 1. Formation and particle size variation. Langmuir 1993, 9, (9), 2301–2309.
45. Roy D; Cambre JN; Sumerlin BS, Sugar-responsive block copolymers by direct RAFT polymerization of unprotected boronic acid monomers. Chem. Commun. 2008, (21), 2477–2479.

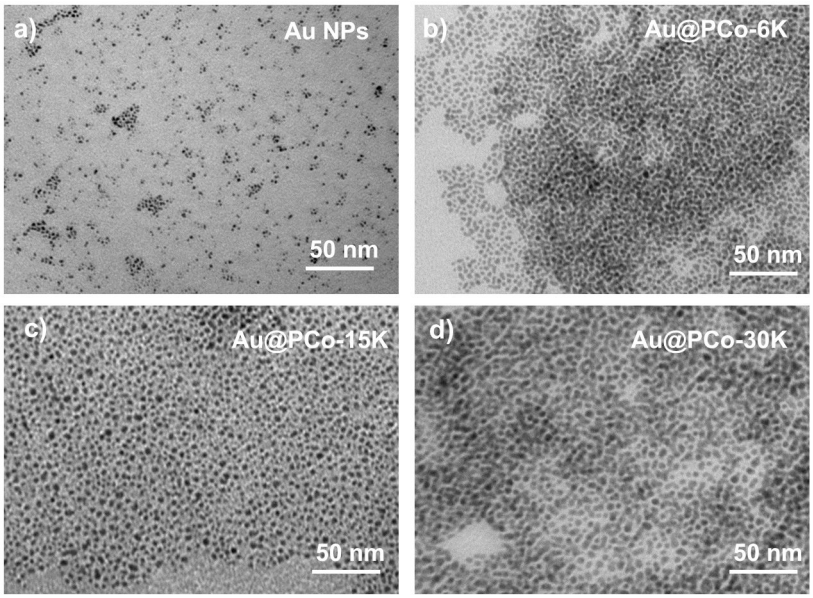

Figure 1.
TEM images of a) Au NPs, b) Au@PCo-6K, c) Au@PCo-15K, and d) Au@PCo-30K.

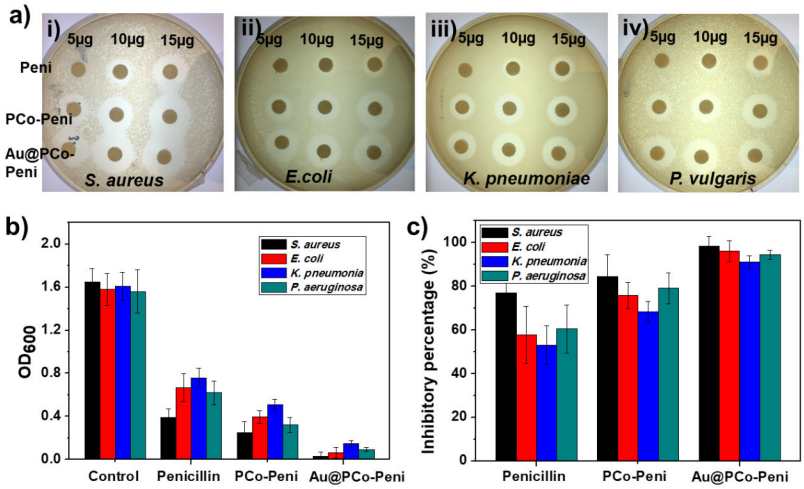

Figure 2.

a) Agar diffusion Disk-diffusion assays of penicillin-G, PCo-Peni conjugates and Au@PCo-Peni NPs against (i) *S.aureus*, (i)*E. coli*, (i) *K. pneumonia*, and (iv) *P. vulgaris.* 30 μL aqueous solution of antimicrobial agents with different weights (5-15 μg) was dropwise added to disks, and the culture dishes were incubated in the oven for 18 h at 28 °C. b) OD_{600} values and c) inhibitory percentage of four bacteria incubated with penicillin-G, PCo-Peni and Au@PCo-Peni NPs, respectively. The tryptic soy broth (TSB) solutions of four different bacteria without any antimicrobial agents were used as the control groups. The 96-well plates were cultured shakily for 12 hours at 37 °C.

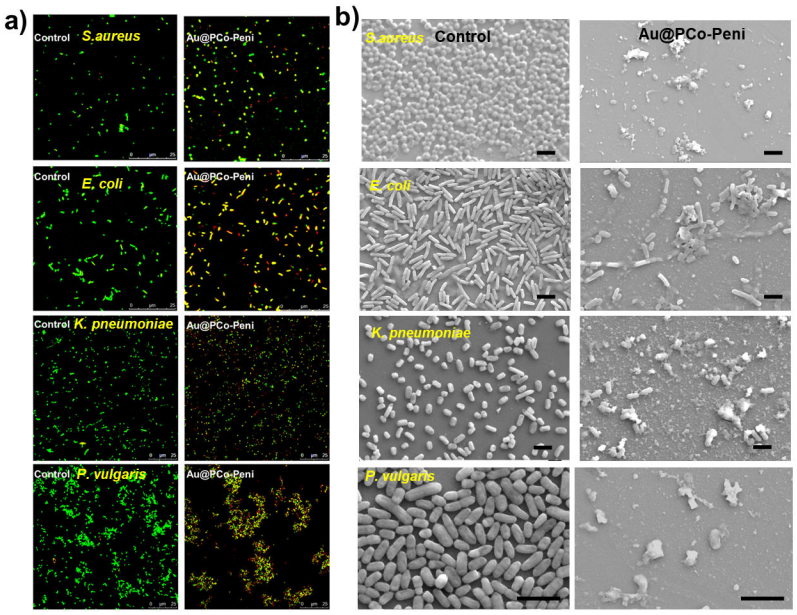

Figure 3.

a) Confocal laser scanning microscopy (CLSM) images and b) scanning electron microscopy (SEM) images of control groups and Au@PCo-Peni NPs against four different bacteria. The concentration of Au@PCo-Peni NPs was 18.5 μg/mL, based on the effective penicillin-G concentration (5 μg/mL) in Au@PCo-Peni NPs. The concentration of bacteria was 1.0×10^6 CFU/mL. For CLSM images, LIVE/DEAD BacLight dye (Bacterial Viability Kit; Invitrogen Inc.) was used to stain the bacteria and check bacteria viability. Green color indicated live bacteria; yellow or red color indicated dead bacteria. For SEM images, all scale bars are 2 μm.

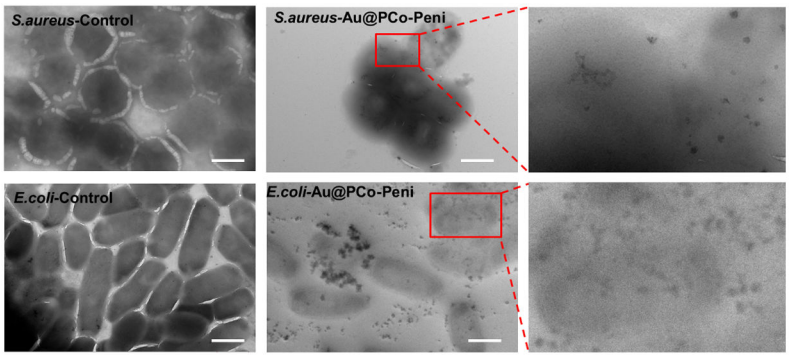

Figure 4.

TEM images of the control and Au@PCo-Peni NPs against *S. aureus* and *E. coli*. The concentration of Au@PCo-Peni NPs was 18.5 μg/mL, based on the effective penicillin-G concentration (5 μg/mL) in Au@PCo-Peni NPs. The concentration of bacteria was 1.0×10^6 CFU/mL. All scale bars are 1 μm.

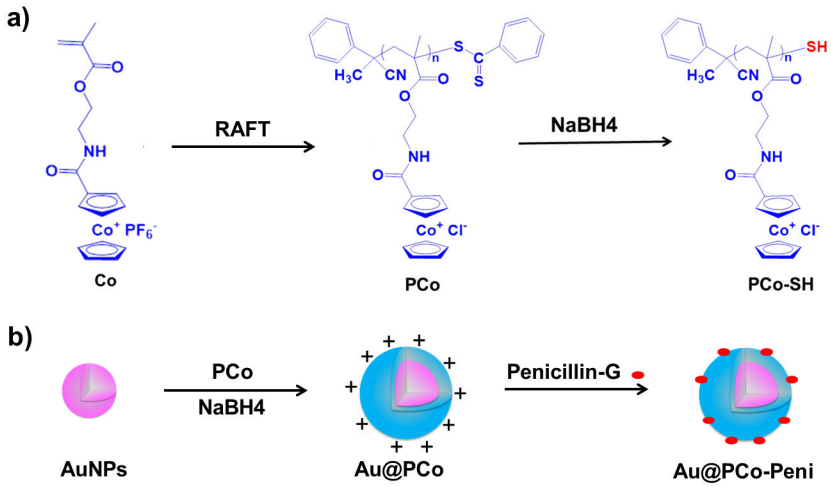

Scheme 1.

a) Synthesis of cationic thiol end-capped cobaltocenium homopolymers by RAFT polymerization and dithioester reduction. b) Synthesis of antimicrobial Au@PCo-Peni nanoparticles by a “grafting-to” approach and a bioconjugation between cationic PCo and anionic β-lactam antibiotic Penicillin-G.

Table 1.

The Minimum Inhibitory Concentrations of penicillin-G, PCo-Peni conjugates, and Au@PCo-Peni NPs against Gram-positive and Gram-negative Bacteria.

Compounds	**Minimum Inhibitory Concentration (MIC, μg/mL)**			
	S. aureus	*E. coli*	*K. pneumonia*	*P. vulgaris*
Penicillin-G	15.8	20.4	23.2	22.6
PCo-Peni	6.4	8.3	8.9	7.8
Au@ PCo-Peni	2.6	4.5	5.4	4.9